Published in final edited form as:
Neuroscience. 2009 November 10; 163(4): 1158–1170. doi:10.1016/j.neuroscience.2009.07.036.

Reticulospinal Neurons in the Pontomedullary Reticular Formation of the Monkey (*Macaca fascicularis*)

Sharleen T. Sakai[1], **Adam G. Davidson**[2], and **John A. Buford**[2,3,4]
Charles Gerfen Dr.
Neuroantomy, Bethesda, MD 20817

[1] Department of Psychology and Neuroscience Program, Michigan State University, East Lansing, MI 48824

[2] Neuroscience Graduate Studies Program, The Ohio State University, Columbus, Ohio 43210

[3] Center for Brain and Spinal Cord Repair, The Ohio State University, Columbus, Ohio 43210

[4] Division of Physical Therapy, School of Allied Medical Professions, The Ohio State University, Columbus, Ohio 43210

Abstract

Recent neurophysiological studies indicate a role for reticulospinal neurons of the pontomedullary reticular formation (PMRF) in motor preparation and goal directed reaching in the monkey. Although the macaque monkey is an important model for such investigations, little is known regarding the organization of the PMRF in the monkey. In the present study, we investigated the distribution of reticulospinal neurons in the macaque. Bilateral injections of wheat germ agglutinin conjugated to horseradish peroxidase (WGA-HRP) were made into the cervical spinal cord. A wide band of retrogradely labeled cells was found in the gigantocellular reticular nucleus (Gi) and labeled cells continued rostrally into the caudal pontine reticular nucleus (PnC) and into the oral pontine reticular nucleus (PnO). Additional retrograde tracing studies following unilateral cervical spinal cord injections of cholera toxin subunit B revealed that there were more ipsilateral (60%) than contralateral (40%) projecting cells in Gi, while an approximate 50:50 contralateral to ipsilateral split was found in PnC and PnO. Reticulospinal neurons in PMRF ranged widely in size from over 50 μm to under 25 μm across the major somatic axis. Labeled giant cells (soma diameters greater than 50 μm) comprised a small percentage of the neurons and were found in Gi, PnC and PnO. The present results define the origins of the reticulospinal system in the monkey and provide an important foundation for future investigations of the anatomy and physiology of this system in primates.

Keywords

cholera toxin; WGA-HRP; immunocytochemistry; substance P; cervical spinal cord

Address correspondence to: Sharleen Sakai, Ph.D. Department of Psychology & Neuroscience Program 218 Giltner Hall Michigan State University East Lansing, MI 48824 Sakai@msu.edu PH: (517) 353-8889 Fax: (517) 432-2744.

INTRODUCTION

The pontomedullary reticular formation (PMRF) in the brainstem is the main source of the reticulospinal tracts (Drew et al., 2004; Kuypers, 1981), and this system plays a well established role in the control of posture and locomotion. A potential role for the reticulospinal system in the control of reaching was suggested by Peterson (1979) based on demonstrated monosynaptic projections to upper limb motoneurons in addition to muscles acting around the neck, and he suggested that follow-up studies in the awake behaving animal would be worthwhile. There are now data confirming that neurons in the PMRF are strongly modulated during reaching (Buford and Davidson, 2004a; 2004b; Schepens et al., 2008; Schepens and Drew, 2004; 2006), and results of electrical stimulation and spike triggered averaging studies also show that the reticulospinal system in the PMRF can recruit upper limb muscles bilaterally (Davidson et al., 2007; Davidson and Buford, 2006; Drew and Rossignol, 1990). Together these findings suggest that the reticulospinal system may play a relatively direct role in the control of limb movements for voluntary reaching in addition to its well established role in control of posture and locomotion.

The reticulospinal system may also have the potential to contribute to recovery of upper limb function after stroke or spinal cord injury. Anatomical tracer studies have shown that the cortical motor areas send numerous bilateral projections to the PMRF in both the cat and the monkey (Keizer and Kuypers 1984, 1989). It is well recognized that the bilateral nature of corticoreticular projections in combination with the bilateral reticulospinal projections positions this system well as an alternative pathway for ipsilateral cortical control of arm movement via corticoreticular projections (Buford, 2008;Canedo, 1997;Denny-Brown, 1966;Drew et al., 2004;Jankowska et al., 2005;Jankowska, 2007;Jankowska and Edgley, 2006;Kuypers, 1981;Rho et al., 1997;Schwerin et al., 2008;Schwerin and Dewald, 2004;Shapovalov, 1973). Lesion studies in the monkey show the fundamental importance of the reticulospinal system in the control of limb movements (Lawrence and Kuypers, 1968), and potentially even digit movements (Nishimura et al., 2007;Pettersson et al., 2007). Lesions of the pyramidal tracts in the cat have also shown the importance of the reticulospinal system as an alternative for control of movement (Alstermark et al., 1983;Jiang and Drew, 1996;Pettersson et al., 1997).

Reticulospinal projections have been described in numerous species, as reviewed by Cruce and Newman (1984). Studies in cats over the years have employed techniques including degeneration (Torvik and Brodal, 1957), retrograde (Tohyama et al., 1979), and anterograde labeling (Holstege, 1991; Matsuyama et al., 1997; 1999; Mitani et al., 1988b). The distribution of the reticulospinal cells has also been described in some detail in the rat (Jones and Yang, 1985; Newman, 1985a; 1985b; Reed et al., 2008) as well as in the opossum (Beran and Martin 1971; Martin and Dom 1971; and Martin et al 1979; 1981). To our knowledge, the only study that used retrograde transport to examine the pontomedullary reticulospinal projections in the macaque is that of Kneisley et al. (1978). However, this study lacked a detailed description of the PMRF and used unconjugated HRP; modern retrograde tracers are more sensitive. The present study describes the distribution of reticulospinal projections based on retrograde tracing with WGA-HRP and CTB. We also present a case with electrophysiological data recorded in a subject with retrogradely labeled reticulospinal cells. To our knowledge, these are the first data on the origins of the reticulospinal system using these techniques in the monkey. Portions of these findings have been presented previously in abstract form (Sakai et al., 2004; Sakai and Buford, 2005; 2007).

EXPERIMENTAL PROCEDURES

Eight adult monkeys (*Macaca fascicularis*) were used in this study. Seven received retrograde tracer injections, and one was used only for examination of the anatomy of the PMRF. The experimental procedures were approved by the IACUC of The Ohio State University and subject care was according to the NIH Guide for the Care and Use of Laboratory Animals.

For retrograde tracing of reticulospinal projection neurons, each monkey was initially anesthetized with ketamine hydrochloride injected intramuscularly (10mg/kg) and then maintained with 2% isoflurane anesthesia inhaled endotracheally. Under aseptic conditions, the animal was then placed in a Kopf stereotaxic apparatus and a laminectomy was performed over the cervical enlargement. The dura mater was incised longitudinally with ophthalmic surgical scissors to expose the spinal cord from the C3 – C5 cervical segments. A 5μl Hamilton syringe was mounted in a custom-built electrode carrier attached to the posterior part of the stereotaxic frame. This arrangement allowed the needle to be adjusted anteroposteriorly and mediolaterally and inserted perpendicular to the surface of the cord at the desired site.

In the first three animals, several pressure injections of 2.5 % wheat germ agglutinin conjugated to horseradish peroxidase (0.5-1.5ul per injection,WGA-HRP; Sigma Chemicals) were made into both sides of the spinal cord at multiple cervical levels in order to broadly define the origins of the reticulospinal tracts. One of these three subjects had been previously implanted with a stainless steel recording chamber and was trained to perform an instructed delay reaching task (case M121-12). This subject had 52 penetrations with recording microelectrodes as described in Davidson and Buford (2006). In the next four animals, 1% cholera toxin subunit B (CTB, Sigma Chemicals) was injected at several locations on one side of the cervical spinal cord in order to determine the ipsilateral and contralateral contributions of the PMRF. The number of injections per case ranged from 5 to 18. In the more medial injection sites, the tracer was deposited at depths of 2.5-mm and 1.5-mm from the surface of the spinal cord, while at the lateral sites a single injection was made 1.5-mm deep only. After each injection, the Hamilton syringe was kept still for 2 minutes to reduce the potential for backflux of tracer into the general cerebrospinal fluid compartment. After the injections, the dura was folded back in place, the opening was covered with GelFilm ™ and the laminectomy packed with Gelfoam ™, and muscles and skin were sutured in layers.

The subjects recovered from anesthesia and received analgesics (Buprenorphine 0.01 mg/kg i.m. BID, ibuprofen 7-10 mg/kg p.o.) during the survival period; and all subjects recovered independent use of all four limbs. Three to four days after the injections, each animal was sedated with ketamine hydrochloride (13 mg/kg i.m.) and then deeply anesthetized with sodium pentabarbitol given i.v. to effect (2-3 ml @ 50 mg/ml). Heparin (10 ml @ 1000 USP units/ml) was administered to prevent coagulation of the blood during perfusion. Each subject was then perfused intracardially with warm phosphate buffered saline, followed by 4% paraformaldehyde, 0.01 M sodium periodate, 0.075 M lysine in phosphate buffer followed by cold 10% and 30% sucrose in phosphate buffer. The brain was removed, immersed in 30% sucrose in phosphate buffer for 2-3 days prior sectioning at 50μm on a freezing microtome.

The normal cytoarchitecture and chemoarchitecture of monkey reticular formation was determined based on analysis of a series of sagittal sections stained for Nissl and substance P immunocytochemistry in one subject that did not receive any retrograde tracer injections. Adjacent series of sections were collected for Nissl staining using cresyl violet and immunocytochemistry using antisera against substance P (raised in rabbit, Immunostar). For the immunocytochemistry, endogenous peroxidase activity was eliminated by incubating the sections first in a hydrogen peroxide mixture. The sections were rinsed in phosphate buffered saline (PBS), blocked in normal goat serum and exposed to the primary antibody to substance

P (1: 6,000 dilution) for 42 hours at 4°C. Sections were then rinsed in PBS, incubated in biotinylated secondary antibody (1:100 dilution), rinsed and incubated in avidin-biotinperoxidase complex (1:50 dilution, Vector Laboratories). The reaction product was visualized using diaminobenzidine and hydrogen peroxidase. Immunocytochemical control procedures included omission of the primary antisera, which abolished any specific labeling. Cytoarchitecture and nomenclature of the monkey brainstem largely followed the descriptions from Paxinos et al. (2000).

In the three subjects where HRP was injected, the tissue was cut in the coronal plane and reacted using tetramethylbenzidine (TMB) as the chromogen with ammonium heptamolybdate as a stabilizing agent, modified from Olucha et al (1985). In subjects where CTB was injected, the tissue was cut in the parasagittal plane and the CTB was identified by immunohistochemistry using a goat anti-CTB antibody (ListBiological Labs, 1:5000) and secondary biotinylated anti-goat IgG (Vector Labs, SK 4600), as described previously (Sakai et al., 2000). The biotinylated antibody was visualized by using the avidin-biotin-immunoperoxidase method with a Vectastain ABC kit (Vector Laboratories) and Vector VIP® substrate kit (Vector Laboratories SK 4600) or diaminobenzidine as the chromagen. Adjacent sections were stained for Nissl substance using cresyl violet.

To define the extent of tracer diffusion at the injection sites, serial horizontal sections through the spinal cord injection sites were plotted onto drawings magnified to 6.5X using an Aus Jena Dokumator. The spread of the tracer including the dark dense core and light diffuse halo were plotted relative to spinal cord gray and white matter tracts.

A selected series of sections for each subject was mapped using the Neurolucida analysis system (Neurolucida 7.5 software, MBF Bioscience, Inc) connected to an Olympus BH-2 microscope equipped with a digital camera (Optronics Microfire), a X-Y-Z encoder and motorized microscope stage connected to a Dell Optiplex computer. WGA-HRP positive cells contained dense blue-black granular reaction product in the neuronal cytoplasm (Mesulam, 1982). Cells labeled with CTB had a fine powdery purple or brown precipitate characteristic of CTB cytoplasmic label (Sakai et al., 2000). Labeled cells were identified using the 20X and 40X microscope objectives. Using Neurolucida software, labeled cells were mapped onto section outlines including the nuclear boundaries of PnO, PnC and Gi as defined from adjacent Nissl-stained sections aligned based on section outlines and blood vessels. Somata of retrogradely labeled cells were counted within these nuclei from a selection of 4 sections using the 20X and 40X microscope objectives. Cell counts were based on analysis of an equal number of parasagittal sections from each side starting at least 0.3 mm from midline. The analyzed sections ranged from 400 to 2200 μm apart and were from comparable parasagittal levels across all cases. Giant cells were separately marked based on soma size exceeding a standard 50 μm diameter circle (adapted from Newman, 1985a). No overestimation correction was made to the cell counts since the cell counts were used for proportional comparison between ipsilateral and contralateral labeling for each case. Photomicrographs were taken using a digital camera (Optronics Microfire) on either a microscope (Olympus BH-2) or macroscope (Olympus SZH). The images were imported into Adobe Photoshop (Version 8.0, San Jose, CA) and if necessary, cropped and adjusted for contrast or brightness. Otherwise, the images were not altered.

RESULTS

Cytoarchitecture of primate PMRF

Based on Nissl stained sections, primate atlases have shown the PMRF only in the coronal plane of section (Szabo and Cowan, 1984; Martin and Bowden 1996; Paxinos et al., 2000). The entire rostrocaudal extent of PMRF can be viewed in parasagittal sections ranging from 1.0-2.0 mm from midline. Thus, this is an ideal orientation in which to view the pattern of

PMRF projections. However, to date there are no detailed descriptions of the macaque PMRF from this plane of section. Therefore, in order to facilitate our description of the distribution of the reticulospinal neurons, we analyzed the primate PMRF in the sagittal plane adapting criteria established for the PMRF subdivisions detailed in transverse sections from the rat (Newman, 1985a; 1985b) and cat (Brodal, 1957) and using coronal atlas descriptions in the monkey (Paxinos et al., 2000). The analysis of the cytoarchitecture of the macaque PMRF was largely based on a series of adjacent sagittal sections stained for Nissl (Fig. 1 A-E) and substance P immunoreactivity. The latter series of sections was used to better identify the medial and dorsal boundary of PMRF in relation to surrounding peptide-rich regions (Hökfelt et al., 2000). Medial to PMRF, the locus coeruleus, raphe nuclei and parabrachial regions are strongly immunoreactive for substance P. In addition, the dorsal and caudal boundaries of the more lightly-stained PMRF are differentiated from the darkly stained nucleus of the solitary tract (Fig. 1F) and hypoglossal nucleus as previously described (Ribeiro-da-Silva and Hökfelt, 2000).

The most prominent feature of the pontomedullary reticular formation is the gigantocellular reticular nucleus (Gi) (Fig. 1). Despite its name, Gi consists of a mixture of multipolar and fusiform neurons with a range of sizes (Fig. 1D). The Gi largely occupies the medial 2/3 of the pontomedullary region. At the rostral extent of Gi, as it transitions into PnC, the density of giant cells visible in the sections decreases. The rostral border of Gi was marked for purposes of analysis by an oblique dorsoventral line beginning approximately 1-mm caudal to abducens and slanting ventrally toward the level of the 7^{th} nerve (Fig. 1). At its most caudal extent, the Gi extends approximately to the level of the obex and overlies the midpoint of the inferior olive. The lateral reticular nucleus (LRt), intermediate reticular nucleus (IRt) and parvicellular reticular nucleus (PCRt) also bound Gi laterally and caudally.

According to Paxinos et al. (2000), Gi can be further divided to include a dorsal division designated dorsal paragigantocellularis (DPGi) and the remaining Gi region, or Gi proper. The DPGi occupied a rectangular region caudal to the abducens nucleus and ventral to prepositus nucleus, vagus and hypoglossal nuclei and consists of mostly multipolar cells of a mixture of sizes (Fig. 1E). Paxinos also assigned three subdivisions to the region of Gi which lies along its ventral border. These subdivisions were gigantocellular nucleus alpha (Giα), gigantocellular nucleus ventral (GiV), and the lateral paragigantocellular nucleus (LPGi). However the boundaries between these three subdivisions were indistinct and difficult to define unequivocally in our specimens. For this reason, our description of the distribution of the reticulospinal projections in the following sections does not differentiate among the subdivisions of Gi.

The caudal pontine reticular nucleus (PnC) is located just rostral to Gi, and partially overlaps the rostral extent of Gi dorsally. Much of PnC is located ventral to the abducens nucleus (6N) and lateral to the raphe nuclei. PnC maintains a similar mediolateral position throughout its rostrocaudal extent and is characterized by the presence of sparsely distributed large and giant multipolar cells. The overall density of the giant cells is lower than that observed in Gi (Fig. 1B). Distinct reticulations are apparent in PnC due to the number of fiber fascicles traversing this region. As noted earlier, although direct comparison of Gi proper with PnC revealed these distinct cytoarchitectonic differences (Fig. 1 B and D), we found that the border between them was indistinct, as the two nuclei gradually transition into each other. At its most rostral extent PnC is replaced by the oral pontine reticular nucleus (PnO), which contains a mixture of large, medium and small multipolar and fusiform cells (Fig. 1A). The cellular packing density appears lower in PnO than in PnC (Fig 1 A and B). Again, there is no distinct boundary apparent at high magnification, but the rostral pole of the abducens nucleus serves as a landmark between the two. Overall, PnO is only lightly immunoreactive for substance P, but the raphe nuclei on the medial boundary of PnO are substance P immunoreactive. Hence the rostral and medial

boundary of PnO can be clearly distinguished. PnO is bounded ventrally by the medial lemiscus and the reticulotegmental nucleus.

Distribution of reticulospinal projections

After establishing general guidelines of the reticular formation cytoarchitecture in the macaque, the reticulospinal projection neurons identified by retrograde tracing were mapped from a total of 7 cases including 3 bilateral injections of WGA-HRP and 4 unilateral injections of CTB into the cervical spinal cord. The gross distribution of labeling was similar across all cases and for both tracers except that bilateral injections resulted in more labeled cells throughout the PMRF.

Case M121-12 received bilateral cervical cord injections of WGA-HRP, and this subject had also been chronically implanted with a recording chamber to allow extracellular recording and stimulation in the PMRF. Analysis of the spinal sections (not shown) indicated a large injection site involving the spinal grey and ventral white matter bilaterally. The dense core is interpreted to the zone of effective uptake for WGA-HRP (Köbbert et al., 2000; Mesulam, 1982), and in this case, there was thorough coverage of the cervical spinal cord at the C4/C5 level. A dark-field photomicrograph of a section containing an electrode track is shown in Fig 2 (also Fig 3 section #53) . Labeled reticulospinal cells were found in PnC and rostral Gi in the area ventral to abducens nucleus (Fig. 3 section #53). This location generally corresponds to stimulation sites that elicited shoulder and arm muscle responses (Davidson and Buford, 2004; 2006). Indeed, the region just below abducens, corresponding to PnC was the site of the most sensitive sites for electrical stimulation to activate the upper trapezius muscles (Davidson and Buford, 2006), and was also the location of most cells that produced significant spike triggered averaging effects (Davidson et al., 2007). As Fig. 3 illustrates, a wide band of labeled cells was observed throughout the pontomedullary region. The greatest density of labeled neurons was observed in Gi, but cells were also labeled in PnC and PnO (not shown). Overall, the area with labeled reticulospinal neurons from the WGA-HRP injection studies corresponds to the region where recording and stimulation sites have demonstrated activity modulated during reaching (Buford et al., 2009; Buford and Davidson, 2004a; Davidson et al., 2007; Davidson and Buford, 2004; 2006).

In order to appreciate the distribution of ipsilateral and contralateral spinal cord projections from the PMRF, the pattern of labeling in representative cases following unilateral cord injections was analyzed. Two of these cases are presented in Figs. 4-5. The third and fourth case showed a similar distribution of the reticulospinal projections to that found in the 2 illustrated cases and are not shown here. The extent of tracer spread was determined from analysis of horizontal sections of the spinal cord. Each injection site had a darkly stained core surrounded by a lighter staining halo that spread peripherally. The zone of effective uptake for CTB may include a portion of the light halo as well as dense core (Craig and Zhang, 2006). Thus, the dense core and halo of the CTB injection sites are depicted as black and gray areas in the diagrams, respectively. In all cases, the CTB spread into the ventral half of the spinal cord and included parts of the ventrolateral and ventromedial funiculi. The CTB injections targeted cervical vertebral level C4 in two cases M0502 (Fig. 4) and M0503 (Fig. 5). Some diffusion of the tracer to the contralateral spinal cord was observed in case M0502. In two other cases not illustrated, CTB was injected at C4-5 unilaterally but in one case, M0604, the halo of the CTB injection site diffused to the contralateral dorsal funiculus.

The greatest density of labeled neurons was observed in Gi, where multipolar as well as fusiform cell types were labeled (Fig. 6A and C). The labeled cells ranged in size from small to giant. Labeled giant cells, neurons with soma diameters greater than 50 μm were sparsely distributed throughout the Gi. Notably, despite the name gigantocellularis, these giant cells accounted for only 1.0% of labeled cells averaged across the 4 cases of ipsilateral cord injections. Therefore, the vast majority of reticulospinal cells in Gi are large to small in size.

For all cell sizes, comparison of the labeling in ipsilateral and contralateral Gi revealed more labeled cells in ipsilateral (60%) than in contralateral Gi (40%) in 3 of the 4 cases (Fig 7). ,In the one remaining case, M0604, 49% of Gi labeling was ipsilateral. The cell labeling extended throughout ipsilateral and contralateral Gi including its most ventral portion dorsal to the inferior olive. This was consistently observed across all cases (Fig. 4 section # 101, 146, 158; Fig. 5 section # 78, 90, 142). The density of cell labeling was not as great in dorsal portions of Gi. Of 143 giant cells found within Gi, about the same proportion (62%) were ipsilateral. No clear topographic pattern was detected in the distribution of giant cell labeling in either ipsilateral or contralateral Gi (Fig. 4-5).

The band of labeled reticulospinal cells continued rostrally into PnC (Figs. 4-5). But in comparison to the density of labeled cell labeling in Gi, the overall density of labeled cells was lower in PnC (Fig. 2 section # 90, 101,138, 146, 158; Fig. 3 section # 78, 90, 142, 154; Fig. 4 section # 87, 99, 164, 179). Fig. 7 shows that the total cell counts decreased ten fold from Gi to PnC. These labeled cells also included a range of sizes and types but most of the reticulospinal cells were medium to large multipolar cells (Fig. 6B). It is notable that relatively more giant cells were labeled in PnC (5.8% averaged across the 4 unilateral injection cases) than in Gi (1.04% averaged across 4 unilateral injection cases), although the actual number of giant cells in PnC (total = 71) is lower than in Gi (total = 143). We also examined the proportion of ipsilateral and contralateral spinal projections arising from PnC as a whole (Fig. 7) and found that these projections are almost equally bilaterally distributed. The proportion was close to 50% in each case, except case M0503 had only about 34% ipsilateral labeling. For 71 giant cells found in PnC, however, 56% were ipsilateral.

The band of labeled reticulospinal cells continues further rostrally and labeled cells were also noted in PnO. These cells are more sparsely distributed than in either PnC or Gi and are located in the caudal half of PnO (Fig. 4 section # 90, 146; Fig. 5 section # 90, 154, 166). In each case, fewer cells were found in PnO than in PnC (Fig 7). The labeled cells in PnO were predominantly medium to large multipolar cells, but a small number of giant cells (total = 22) were also observed. Reticulospinal cells arise from both the contralateral and ipsilateral PnO. However, in 3 of the four cases, more PnO cells (66%) were labeled contralaterally (Fig 7). However, of the 22 labeled giant cells in PnO, 15 (68%) were ipsilateral.

A chi-square analysis revealed a significant effect of laterality of cell labeling by nucleus ($\chi^2 = 269$, $P < 0.001$). As shown in Fig 7, there were more ipsilateral cells in Gi, about a 50:50 spilt in PnC, and more contralateral cells in PnO. However, a similar analysis of laterality and number of labeled giant cells failed to reveal a significant effect ($\chi^2 = 1.1$, $P = 0.57$). Overall, 61% of giant cells were found ipsilaterally.

DISCUSSION

In the present study, we found that the PMRF gives rise to dense bilateral reticulospinal projections in the monkey. A wide swath of labeled cells was found primarily in Gi, and this labeling continued rostrally into PnC and into the caudal PnO. Although a greater number of giant cells were labeled in Gi than PnC, proportionally more giant cells were found in PnC. In addition, the proportion of ipsilateral reticulospinal cells exceeded the contralateral cells in Gi whereas the ipsilateral and contralateral reticulospinal contributions arising from PnC were similar, and projections from PnO were more contralateral. These results indicate that the distribution of descending reticulospinal projection neurons varies regionally.

Primate PMRF

The cytoarchitecture of the reticular formation has been examined in several mammalian species including the opossum (Martin et al., 1981), the cat (Brodal, 1957), and rat (Newman,

1985a; 1985b), but relatively little is known regarding the macaque PMRF. Here, we found the cytoarchitectonic characteristics of PMRF described in other mammals (Voogd et al., 1998) can be applied to the monkey. In particular, the relative location, boundaries and characteristics of neuronal size and types in Gi, PnO and PnC described by Brodal in the cat (1957) can be readily applied to the monkey.

Despite the general similarities in the cellular characteristics and relative location of PnO, PnC and Gi between these species, the nuclear subdivisions in Gi appear to be less distinct in the macaque. Within the primate Gi, the ventral subdivisions of Giα and GiV identified by Paxinos et al. (2000) appear to largely correspond to nucleus reticularis magnocellularis in the cat (Berman, 1968) and nucleus reticularis magnocellularis alpha and beta in the rat (Newman, 1985a). In our material, these nuclei could not be clearly and consistently distinguished in the parasagittal plane. This may be because the cellular packing density overall in PMRF appears to be less in the primate brain, perhaps due to a relative increase in overall brain volume in comparison to the rat or cat. Indeed, several more subdivisions of PMRF have been identified by Newman in the rat (1985a; 1985b) than we were able to clearly distinguish in the primate pontomedullary region. For these reasons, we confined our description of the reticulospinal projections to the PnO, PnC and Gi. There is some evidence that the reticulospinal system may, like the corticospinal system, have more influence over distal muscles in the monkey than in the cat or rat (Baker and Riddle, 2007; Pettersson et al., 2007). In the present study, we cannot see any obvious changes in cytoarchitectural organization to accompany this potentially expanded functional role.

It is not known if variation in cell types and sizes in the PMRF correspond to hodological differences. Giant cells in both Gi and PnC have been noted across a number of species (Voogd et al., 1998). In PnC, these cells are thought to be a critical relay in the acoustic startle response for rats and cats (Lingenhohl and Friauf, 1994; Yeomans and Frankland, 1996) and for an escape response in fish (Bosch et al, 2001). Lingenhohl and Friauf demonstrated in the rat, the PnC giant cells which were likely to be reticulospinal cells receive bilateral innervation from dorsal cochlear nuclei and the superior olive (1994). These elements are hypothesized to constitute the critical components of an acoustic startle pathway (Lingenhohl and Friauf, 1994; Yeomans and Frankland, 1996).

In addition to giant cells, the PMRF includes numerous multipolar as well as fusiform cells with a range of sizes that were labeled as reticulospinal cells. The fusiform cells were more common in the lateral portions of Gi. Based on their location, one might propose that the fusiform cells are more likely to contribute to the lateral reticulospinal tract (Peterson et al., 1975). Whether this is the case awaits further study.

Reticulospinal projections are bilateral

As previously noted, the reticulospinal system is thought be a system that remains highly conserved across species (Voogd et al., 1998). Previous studies in the cat (Mitani et al., 1988a; Tohyama et al., 1979; Torvik and Brodal, 1957), and rat (Mitani et al., 1988a; Tohyama et al., 1979; Torvik and Brodal, 1957) have described bilateral reticulospinal projections noting that the spinal projections from Gi have a weak ipsilateral predominance. In the present study, we found an approximate 60:40 split between the ipsilateral and contralateral Gi cells labeled by spinal cord injections as averaged from our 4 unilateral injection cases. In addition, we found labeled reticulospinal cells bilaterally in PnC, with about a 50:50 split, and about 60% contralateral projections from PnO. These findings are comparable with earlier studies in a number of different species, although quantitative analysis of laterality in these earlier reports is lacking. In the rat, Jones and Yang (1985) noted that more large and giant reticulospinal cells in the medulla were labeled ipsilaterally and more medium to large reticulospinal cells in the caudal pons were labeled contralaterally. Newman (1985a; 1985b) also noted that in rats,

reticulospinal projections from Gi are strongly ipsilateral but ipsilateral and contralateral descending projections from PnO did not differ. Also in agreement with our findings, Tohyama and others (1979) found in the cat that reticulospinal projections were mostly ipsilateral in Gi. These authors, like Newman (1985a; 1985b), further subdivided PnC and PnO into several parts. Because these subdivisions were not found in the macaque, comparison between these data sets is problematic. Finally, in the macaque, Kneisley and colleagues (1978) noted that reticulospinal projections were bilateral but were predominantly ipsilateral. They did not elaborate on laterality projection differences from Gi, PnC, and PnO and did not quantify the predominance of ipsilateral reticulospinal projections.

While retrograde tracing experiments are ideal for demonstrating the distribution of projection cells of origin, such experiments fail to reveal complete details of projection systems and questions remain regarding precise interpretation of the effective injection site (Craig and Zhang, 2006; Köbbert et al., 2000). Both WGA-HRP and CTB are thought to be taken up actively by nerve terminals and cut axons, but may also be passively transported by fibers of passage (Chen and Aston-Jones, 1995). While it is possible that in the present study some of the reticulospinal labeling may be the result of uptake by damaged fibers, we believe that the problem is limited since (1) a relatively small number of penetrations were made under stereotaxic control with a small (30 ga.) needle and (2) the animals recovered independent use of all four limbs after the injections. In addition, although both tracers also transport in an anterograde manner (Köbbert et al., 2000), we noted no anterograde labeling in the cuneate nucleus. Such labeling would be present if there was uptake by fibers of passage since the injection needle penetrated the fasciculus cuneatus in order to reach the target site. This suggests that intact terminals were most likely the primary mode of uptake in the present results. Finally, it has been noted that WGA-HRP can be transported trans-synaptically, especially in active synapses (Alstermark and Kummel, 1986; Köbbert et al., 2000). To the extent that commissural interneurons are a strong target of reticulospinal cells (Jankowska, 2007; Jankowska et al., 2003), this could have contributed to the labeling described here. However, since WGA-HRP was only used as the tracer in the one case (M121-12) involving bilateral injections into the cervical cord and these data were not used for evaluating the laterality of the reticulopinal projections, the possibility of transneuronal labeling does not alter our findings.

In the present study, the retrograde tracer CTB was used to determine the laterality of the reticulospinal projections. While the current methodology using CTB and WGA-HRP is more sensitive in revealing projection cells than that found using HRP only or degeneration methods (Bruce and Grofova, 1992; Köbbert et al., 2000), the retrograde tracing method is limited in revealing details of fiber trajectories and axonal collateralization. Based on tracing of single axons after anterograde injections of PHA-L into PnO and PnC in the cat, Matsuyama et al. (1997; 1999) determined that pontine reticulospinal neurons tend to descend ipsilaterally in the medial reticulospinal tracts in the ventral funiculus and deliver collaterals to both sides of the spinal cord at cervical, thoracic, and lumbar levels. By recording from identified reticulospinal cells and antidromically stimulating from various locations, Peterson et al. (1975) also concluded that reticulospinal neurons from PnC and the rostral/dorsal part of Gi are most likely to descend ipsilaterally in the medial reticulospinal tract, and usually terminate on both sides of the spinal cord. In the more lateral and ventral parts of Gi, Peterson et al. (1975) found it more likely to locate neurons descending in the lateral reticulospinal tracts. Again the majority of these were found to descend and terminate ipsilaterally, but a small fraction (~5%) appeared to decussate in the brainstem and then descend and terminate contralaterally. These neurons of the lateral reticulospinal tract do not appear to ramify as widely among segmental levels, nor do they seem as likely to decussate in the spinal segments (Matsuyama et al., 2004; Peterson et al., 1975; 1978) instead they appear to terminate on the same side that they descend.

Based on the retrograde tracing method used in the present study, we cannot determine if the axons from a labeled PMRF cells traversed the medial or lateral reticulospinal tract. Unlike previous work by Tohyama and colleagues (1979), our spinal cord injections were not limited to either the ventral or lateral funiculus. Thus, we are unable to provide further details on the descending course of the medial and lateral reticulospinal tracts based on the data presented. However, contributions to the reticulospinal tracts may be surmised based on the location of the reticulospinal cells. The more caudal and lateral portions of Gi are thought to be the origin of cells descending in the lateral reticulospinal tracts (Matsuyama et al., 2004; Peterson et al., 1978; Peterson et al., 1975), whereas the medial reticulospinal tracts are thought to originate from PnO, PnC, and Gi proper (Holstege and Kuypers, 1982; Matsuyama et al., 1997; 1999; Peterson et al., 1975). The lateral reticulospinal tract appears to be largely unilateral and is much more ipsilateral than contralateral. This suggests that the higher proportion of ipsilateral cells found in Gi might be due to the presence of cells from the lateral reticulospinal tract adding to the proportion of ipsilateral fibers. Hence, the higher proportion of contralateral projections found in PnO and PnC may be attributed to the medial reticulospinal tracts, and the 60:40 split found in Gi may include axons of cells traversing the lateral and medial reticulospinal tracts.

Functional implications

Neurons in the PMRF are hypothesized to play a role in a wide variety of functions including arousal, autonomic functions, sensory processing, and movement (Brodal, 1981; Drew et al., 2004; Holstege, 1991; Kuypers, 1981; Peterson et al., 1979; Wilson and Peterson, 1981). In studies of motor function, microstimulation within the PMRF has resulted in bilateral recruitment of upper limb muscles in the monkey (Davidson et al., 2007; Davidson and Buford, 2006). In these studies, the head was restrained and the subject was sitting, so there are no data on whether head or leg muscles were also recruited. In a study with the head of the monkey unrestrained, electrical stimulation in the PMRF resulted in head movements that were thought to be associated with gaze shifts (Freedman and Quessy, 2004; Quessy and Freedman, 2004). Shapovalov's work indicates that primate reticulospinal outputs can affect lumbar motoneurons (Shapovalov, 1972). In cats, where all four limbs can more readily be studied in freely moving subjects, it is clear that PMRF outputs can affect all four limbs (Drew and Rossignol, 1990). We suspect that the output of the PMRF can affect all four limbs in the primate as well.

In the upper limbs, the most common result of electrical stimulation in the PMRF is facilitation of ipsilateral flexors and contralateral extensors with simultaneous suppression of ipsilateral extensors and contralateral flexors (Davidson et al., 2007; Davidson and Buford, 2006). Neural activity in the PMRF in association with reaching in the cat (Schepens et al., 2008) and primate (Buford et al., 2009) is also consistent with this result. The reticulospinal projection system may provide an important anatomical substrate for recovery of forearm function following stroke, where similar flexor/extensor synergies are often observed (Dewald et al., 1995; Schwerin et al., 2008). Detailing the mechanisms by which cortical projections to the reticulospinal system might mediate such effects will require further investigation.

ACKNOWLEDGEMENTS

We thank Stephanie Moran and Sheri Sanders for excellent technical assistance. We also thank Wendy Herbert, Jake Banks, Brooke Kleinert and Sarah Hutton for their help during the data collection and Lynnette Montgomery for critical reading of the manuscript. This work was supported by NIH NINDS R01 NS037822 to JAB. Present address for Dr. Davidson: Dept. of Neurobiology and Anatomy, University of Rochester Medical Center, Box 603, 601 Elmwood Ave., Rochester, NY 14642

LIST OF ABBREVIATIONS

10N, vagus nucleus
12N, hypoglossal nucleus

12n, root of hypoglossal nerve
5n, root of trigeminal nerve
6N, abducens nucleus
7n, root of facial nerve
7N, facial nucleus
BC, brachium conjunctive
Cu, cuneate nucleus
DPGi, dorsal paragigantocellular nucleus
Gi, gigantocellular reticular nucleus
Giα, gigantocellular nucleus, alpha
GiV, gigantocellular nucleus, ventral
gr, gracile fasciculus
icp, inferior cerebellar peduncle
IO, inferior olive
IRt, intermediate reticular nucleus
IVe, inferior vestibular nucleus
LC, locus coeruleus
LRt, lateral reticular nucleus
LPGi, lateral paragigantocellular nucleus
LVe, lateral vestibular nucleus
m5, motor root of trigeminal nerve
mlf, medial longitudinal fasciculus
MRt, medial reticular nucleus
MVe, medial vestibular nucleus
PCRt, parvicellular reticular nucleus
Pn, pontine nuclei
PnC, pontine reticular nucleus, caudal
PnO, pontine reticular nucleus, oralis
PnR, pontine raphe nucleus
Pr, prepositus nucleus
Pr5, principal sensory trigeminal nucleus
Py, pyramidal tract
RMg, raphe magnus nucleus
RtTg, reticulotegmental nucleus of the pons
Scp, superior cerebellar peduncle
SO, superior olive
Sol, nucleus of solitary tract
Sol, solitary tract
Sp5, spinal trigeminal nucleus
VRt, ventral reticular nucleus

REFERENCES

Alstermark B, Kummel H. Transneuronal labelling of neurones projecting to forelimb motoneurones in cats performing different movements. Brain Res 1986;376:387–391. [PubMed: 3730842]

Alstermark B, Pinter M, Sasaki S. Brainstem relay of disynaptic pyramidal EPSPs to neck motoneurons in the cat. Brain Res 1983;259:147–150. [PubMed: 6297666]

Baker SN, Riddle CN. The macaque reticulospinal tract forms monosynaptic connections with motoneurons in the cervical spinal cord controlling distal arm and hand muscles. Soc.Neurosci.Abstr 2007;191.3

Beran RL, Martin GF. Reticulospinal fibers of the opossum, Didelphis virginiana. I. Origin. J Comp Neurol 1971;141:453–465. [PubMed: 4101679]

Berman, AL. The brain stem of the cat: a cytoarchitectonic atlas with stereotaxic coordinates. University of Wisconsin Press; Madison, WI: 1968.

Bosch T, Maslam S, Roberts B. Fos-like immunohistochemical identification of neurons active during the startle response of the rainbow trout. J Comp Neurol 2001;439:306–314. [PubMed: 11596056]

Brodal, A. The Henderson Trust Lectures. Oliver & Boyd; Edinburgh: 1957. The Reticular Formation of the Brain Stem. Anatomical Aspects and Functional Correlations..

Brodal, A. Neurological anatomy in relation to clinical medicine. Oxford Univ. Press; New York: 1981.

Bruce K, Grofova I. Notes on a light and electron microscopic double-labeling method combining anterograde tracing with Phaseolus vulgaris leucoagglutinin and retrograde tracing with cholera toxin subunit B. J. Neurosci. Methods 1992;45:23–33. [PubMed: 1283431]

Buford, JA. Reticulospinal System.. In: Squire, Larry, et al., editors. The New Encyclopedia of Neuroscience. Elsevier; 2008.

Buford JA, Davidson AG. Movement-related and preparatory activity in the reticular formation during a bilateral reaching task. 2004aSociety for NeuroscienceWashington, DC Program No.918.4.2004 Abstract Viewer/Itinerary Planner, Online 11-1-2004a.

Buford JA, Davidson AG. Movement-related and preparatory activity in the reticulospinal system of the monkey. Exp. Brain Res 2004b;159:284–300. [PubMed: 15221165]

Buford JA, Herbert WJ, Davidson AG. Neural activity in the pontomedullary reticular formation of the monkey related to reaching for a bilateral instructed delay task. J Neurophysiol. 2009(in review)

Canedo A. Primary motor cortex influences on the descending and ascending systems. Prog. Neurobiol 1997;51:287–335. [PubMed: 9089791]

Chen S, Aston-Jones G. Evidence that cholera toxin B subunit (CTb) can be avidly taken up and transported by fibers of passage. Brain Res 1995;674:107–111. [PubMed: 7773677]

Craig AD, Zhang ET. Retrograde analyses of spinothalamic projections in the macaque monkey: input to posterolateral thalamus. J. Comp Neurol 2006;499:953–964. [PubMed: 17072831]

Cruce WLR, Newman DB. Evolution of Motor Systems: The Reticulospinal Pathways. Amer. Zool 1984;24:733–753.

Davidson AG, Buford JA. Motor outputs from the primate reticular formation to shoulder muscles as revealed by stimulus triggered averaging. J. Neurophysiol 2004;92:83–95. [PubMed: 15014106]

Davidson AG, Buford JA. Bilateral actions of the reticulospinal tract on arm and shoulder muscles in the monkey: stimulus triggered averaging. Exp. Brain Res 2006;173:25–39. [PubMed: 16506008]

Davidson AG, Schieber MH, Buford JA. Bilateral spike-triggered average effects in arm and shoulder muscles from the monkey pontomedullary reticular formation. J. Neurosci 2007;27:8053–8058. [PubMed: 17652596]

Denny-Brown, D. The cerebral control of movement. Charles C Thomas; Springfield, IL: 1966.

Dewald JP, Pope PS, Given JD, Buchanan TS, Rymer WZ. Abnormal muscle coactivation patterns during isometric torque generation at the elbow and shoulder in hemiparetic subjects. Brain 1995;118(Pt 2): 495–510. [PubMed: 7735890]

Drew T, Prentice S, Schepens B. Cortical and brainstem control of locomotion. Prog. Brain Res 2004;143:251–261. [PubMed: 14653170]

Drew T, Rossignol S. Functional organization within the medullary reticular formation of intact unanesthetized cat. I. Movements evoked by microstimulation. J. Neurophysiol 1990;64:767–781. [PubMed: 2230923]

Freedman EG, Quessy S. Electrical Stimulation of rhesus monkey nucleus reticularis gigantocellularis: II. Effects on metrics and kinematics of ongoing gaze shifts. Exp. Brain Res 2004;156:357–376. [PubMed: 14985900]

Hökfelt T, Arvidsson U, Cullheim S, Millhorn D, Nicholas AP, Pieribone V, Seroogy K, Ulfhake B. Multiple messengers in descending serotonin neurons: localization and functional implications. J. Chem. Neuroanat 2000;18:75–86. [PubMed: 10708921]

Holstege G. Descending Motor Pathways and the Spinal Motor System - Limbic and Nonlimbic Components. Progress in Brain Research 1991;87:307–421. [PubMed: 1678191]

Holstege G, Kuypers HG. The anatomy of brain stem pathways to the spinal cord in cat. A labeled amino acid tracing study. Prog. Brain Res 1982;57:145–175. [PubMed: 7156396]

Jankowska E. Spinal interneuronal networks in the cat: Elementary components. Brain Res. Rev 2007;57:46–55. [PubMed: 17884173]

Jankowska E, Cabaj A, Pettersson LG. How to enhance ipsilateral actions of pyramidal tract neurons. J. Neurosci 2005;25:7401–7405. [PubMed: 16093391]

Jankowska E, Edgley SA. How can corticospinal tract neurons contribute to ipsilateral movements? A question with implications for recovery of motor functions. Neuroscientist 2006;12:67–79. [PubMed: 16394194]

Jankowska E, Hammar I, Slawinska U, Maleszak K, Edgley SA. Neuronal basis of crossed actions from the reticular formation on feline hindlimb motoneurons. J. Neurosci 2003;23:1867–1878. [PubMed: 12629191]

Jiang W, Drew T. Effects of bilateral lesions of the dorsolateral funiculi and dorsal columns at the level of the low thoracic spinal cord on the control of locomotion in the adult cat. I. Treadmill walking. J. Neurophysiol 1996;76:849–866. [PubMed: 8871204]

Jones BE, Yang TZ. The efferent projections from the reticular formation and the locus coeruleus studied by anterograde and retrograde axonal transport in the rat. J. Comp Neurol 1985;242:56–92. [PubMed: 2416786]

Keizer K, Kuypers HG. Distribution of corticospinal neurons with collaterals to the lower brain stem reticular formation in monkey (Macaca fascicularis). Exp. Brain Res 1989;74:311–318. [PubMed: 2924851]

Keizer K, Kuypers HG. Distribution of corticospinal neurons with collaterals to lower brain stem reticular formation in cat. Exp. Brain Res 1989;54:107–120. [PubMed: 6698141]

Kneisley LW, Biber MP, LaVail JA. A study of the origin of brain stem projections to monkey spinal cord using the retrograde transport method. Exp. Neurol 1978;60:116–139. [PubMed: 77794]

Köbbert C, Apps R, Bechmann I, Lanciego JL, Mey J, Thanos S. Current concepts in neuroanatomical tracing. Prog. Neurobiol 2000;62:327–351. [PubMed: 10856608]

Kuypers HG. Anatomy of descending pathways. Handbook of Physiology 1981:597–666.666Bethesda, MD Sect. I. The Nervous System. Vol. II. Motor Control, pt 1., vol. II, Motor Control, pt. 1. Am. Physiol. Soc.

Lawrence DG, Kuypers HG. The functional organization of the motor system in the monkey. II. The effects of lesions of the descending brain-stem pathways. Brain 1968;91:15–36. [PubMed: 4966860]

Lemon RN. Descending Pathways in Motor Control. Annual Review of Neuroscience 2008;31:195–218.

Lingenhohl K, Friauf. Giant neurons in the rat reticular formation: a sensorimotor interface in the elementary acoustic startle circuit? J Neurosci 1994;14:1176–1194. [PubMed: 8120618]

Martin GF, Cabana T, Humbertson AO Jr. Laxson LC, Panneton WM. Spinal projections from the medullary reticular formation of the North American opossum: evidence for connectional heterogeneity. J. Comp Neurol 1981;196:663–682. [PubMed: 6110678]

Martin GF, Dom R. Reticulospinal fibers of the opossum, Didelphis virginiana. II. Course, caudal extent and distribution. J Comp Neurol 1971;141:467–483. [PubMed: 4101680]

Martin GF, Humbertson AO Jr, Laxson LC, Panneton WM, Tschismadia I. Spinal projections from the mesencephalic and pontine reticular formation in the North American Opossum: a study using axonal transport techniques. J Comp Neurol 1979;187:373–399. [PubMed: 489785]

Martin RF, Bowden DM. A stereotaxic template atlas of the macaque brain for digital imaging and quantitative neuroanatomy. Neuroimage 1996;4:119–150. [PubMed: 9345504]

Matsuyama K, Mori F, Kuze B, Mori S. Morphology of single pontine reticulospinal axons in the lumbar enlargement of the cat: a study using the anterograde tracer PHA-L. J. Comp Neurol 1999;410:413–430. [PubMed: 10404409]

Matsuyama K, Mori F, Nakajima K, Drew T, Aoki M, Mori S. Locomotor role of the corticoreticular-reticulospinal-spinal interneuronal system. Prog. Brain Res 2004;143:239–249. [PubMed: 14653169]

Matsuyama K, Takakusaki K, Nakajima K, Mori S. Multi-segmental innervation of single pontine reticulospinal axons in the cervico-thoracic region of the cat: anterograde PHA-L tracing study. J. Comp Neurol 1997;377:234–250. [PubMed: 8986883]

Mesulam, MM. Tracing neural connections with horseradish peroxidase. Wiley; New York: 1982.

Mitani A, Ito K, Mitani Y, McCarley RW. Descending projections from the gigantocellular tegmental field in the cat: cells of origin and their brainstem and spinal cord trajectories. J. Comp Neurol 1988a; 268:546–566. [PubMed: 2451685]

Mitani A, Ito K, Mitani Y, McCarley RW. Morphological and electrophysiological identification of gigantocellular tegmental field neurons with descending projections in the cat: I. Pons. J. Comp Neurol 1988b;268:527–545. [PubMed: 3356804]

Newman DB. Distinguishing rat brainstem reticulospinal nuclei by their neuronal morphology. I. Medullary nuclei. J. Hirnforsch 1985a;26:187–226. [PubMed: 2410489]

Newman DB. Distinguishing rat brainstem reticulospinal nuclei by their neuronal morphology. II. Pontine and Mesencephalic nuclei. J. Hirnforsch 1985b;26:385–418. [PubMed: 4067279]

Nishimura Y, Onoe H, Morichika Y, Perfiliev S, Tsukada H, Isa T. Time-dependent central compensatory mechanisms of finger dexterity after spinal cord injury. Science 2007;318:1150–1155. [PubMed: 18006750]

Olucha F, Martinez-Garcia F, Lopez-Garcia C. A new stabilizing agent for the tetramethyl benzidine (TMB) reaction product in the histochemical detection of horseradish peroxidase (HRP). J. Neurosci. Methods 1985;13:131–138. [PubMed: 3999803]

Paxinos, G.; Huang, XF.; Toga, AW. The Rhesus Monkey Brain in Stereotaxic Coordinates. Academic Press; San Diego: 2000.

Peterson BW. Reticulospinal projections to spinal motor nuclei. Ann. Rev. Physiol 1979;41:127–140. [PubMed: 373586]

Peterson BW, Maunz RA, Pitts NG, Mackel RG. Patterns of projection and branching of reticulospinal neurons. Exp. Brain Res 1975;23:333–351. [PubMed: 1183508]

Peterson BW, Pitts NG, Fukushima K. Reticulospinal connections with limb and axial motoneurons. Exp. Brain Res 1979;36:1–20. [PubMed: 467530]

Peterson BW, Pitts NG, Fukushima K, Mackel R. Reticulospinal excitation and inhibition of neck motoneurons. Exp. Brain Res 1978;32:471–489. [PubMed: 689126]

Pettersson LG, Alstermark B, Blagovechtchenski E, Isa T, Sasaski S. Skilled digit movements in feline and primate--recovery after selective spinal cord lesions. Acta Physiol (Oxf) 2007;189:141–154. [PubMed: 17250565]

Pettersson LG, Lundberg A, Alstermark B, Isa T, Tantisira B. Effect of spinal cord lesions on forelimb target-reaching and on visually guided switching of target-reaching in the cat. Neurosci. Res 1997;29:241–256. [PubMed: 9436650]

Quessy S, Freedman EG. Electrical stimulation of rhesus monkey nucleus reticularis gigantocellularis: I. Characteristics of evoked head movements. Exp. Brain Res 2004;156:342–356. [PubMed: 14985893]

Reed WR, Shum-Siu A, Magnuson DS. Reticulospinal pathways in the ventrolateral funiculus with terminations in the cervical and lumbar enlargements of the adult rat spinal cord. Neuroscience 2008;151:505–517. [PubMed: 18065156]

Rho MJ, Cabana T, Drew T. Organization of the projections from the pericruciate cortex to the pontomedullary reticular formation of the cat: a quantitative retrograde tracing study. J. Comp Neurol 1997;388:228–249. [PubMed: 9368839]

Ribeiro-da-Silva A, Hökfelt T. Neuroanatomical localisation of Substance P in the CNS and sensory neurons. Neuropeptides 2000;34:256–271. [PubMed: 11049730]

Sakai, ST.; Buford, JA. The distribution of corticoreticular and reticulospinal projections in the macaque monkey.. Neuroscience Meeting Planner.; Washington, DC: Society for Neuroscience. 2005. Program No.181.1.20052005.Online

Sakai, ST.; Buford, JA. The distribution of supplementary motor area and premotor area projections to reticulospinal neurons in the macaque monkey.. Neuroscience Meeting Planner.; San Diego, CA: Society for Neuroscience. 11-12-2007; 2007. Program No.191.2.2007Online 2007

Sakai, ST.; Buford, JA.; Davidson, AG. The distribution of reticulospinal neurons in the macaque monkey.. Neuroscience Meeting Planner.; Washington DC.Society for Neuroscience. 2004. Program No.755.16.20042004.Online

Sakai ST, Stepniewska I, Qi HX, Kaas JH. Pallidal and cerebellar afferents to pre-supplementary motor area thalamocortical neurons in the owl monkey: a multiple labeling study. J Comp Neurol 2000;417:164–180. [PubMed: 10660895]

Schepens B, Drew T. Independent and convergent signals from the pontomedullary reticular formation contribute to the control of posture and movement during reaching in the cat. J. Neurophysiol 2004;92:2217–2238. [PubMed: 15175364]

Schepens B, Drew T. Descending signals from the pontomedullary reticular formation are bilateral, asymmetric, and gated during reaching movements in the cat. J. Neurophysiol 2006;96:2229–2252. [PubMed: 16837662]

Schepens B, Stapley P, Drew T. Neurons in the pontomedullary reticular formation signal posture and movement both as an integrated behavior and independently. J. Neurophysiol 2008;100:2235–2253. [PubMed: 18632892]

Schwerin S, Dewald JP, Haztl M, Jovanovich S, Nickeas M, MacKinnon C. Ipsilateral versus contralateral cortical motor projections to a shoulder adductor in chronic hemiparetic stroke: implications for the expression of arm synergies. Exp. Brain Res 2008;185:509–519. [PubMed: 17989973]

Schwerin SC, Dewald JPA. Ipsilateral hemisphere control of upper extremity muscles following stroke using transcranial magnetic stimulation. 2004Society for Neuroscience Program Number 878.4.2004 abstract Viewer/Itinerary Planner. 10-27-2004.

Shapovalov AI. Extrapyramidal monosynaptic and disynaptic control of mammalian alpha-motoneurons. Brain Res 1972;40:105–115. [PubMed: 4624482]

Shapovalov, AI. Extrapyramidal control of primate motoneurons.. In: Desmedt, JE., editor. Human Reflexes, Pathophysiology of Motor Systems, Methodology of Human Reflexes. Vol. 3. Karger; Basel: 1973. p. 145-158.

Szabo J, Cowan WM. A stereotaxic atlas of the brain of the cynomolgus monkey (Macaca fascicularis). J. Comp Neurol 1984;222:265–300. [PubMed: 6365984]

Tohyama M, Sakai K, Salvert D, Touret M, Jouvet M. Spinal projections from the lower brain stem in the cat as demonstrated by the horseradish peroxidase technique. I. Origins of the reticulospinal tracts and their funicular trajectories. Brain Res 1979;173:383–403. [PubMed: 487101]

Torvik A, Brodal A. The origin of reticulospinal fibers in the cat; an experimental study. Anat. Rec 1957;128:113–137. [PubMed: 13458831]

Voogd, J.; Nieuwenhuys; vanDoner, PAM.; ten Donkelaar, HJ. Mammals.. In: Nieuwenhuys, R.; ten Donkelaar, HJ.; Nicholson, C., editors. The Central Nervous System of Vertebrates. Vol. 3. Springer-Verlag; 1998. p. 1637-2097.

Wilson VJ, Peterson BW. Vestibulospinal and reticulospinal systems. Handbook of Physiology 1981:667–702.702Bethesda, MD Sect 1. The Nervous System, vol. II. Motor Control, pt. 1. Am. Physiol. Soc.

Yeomans J, Frankland P. The acoustic startle reflex: neurons and connections. Brain Res Rev 1996;21:301–314. [PubMed: 8806018]

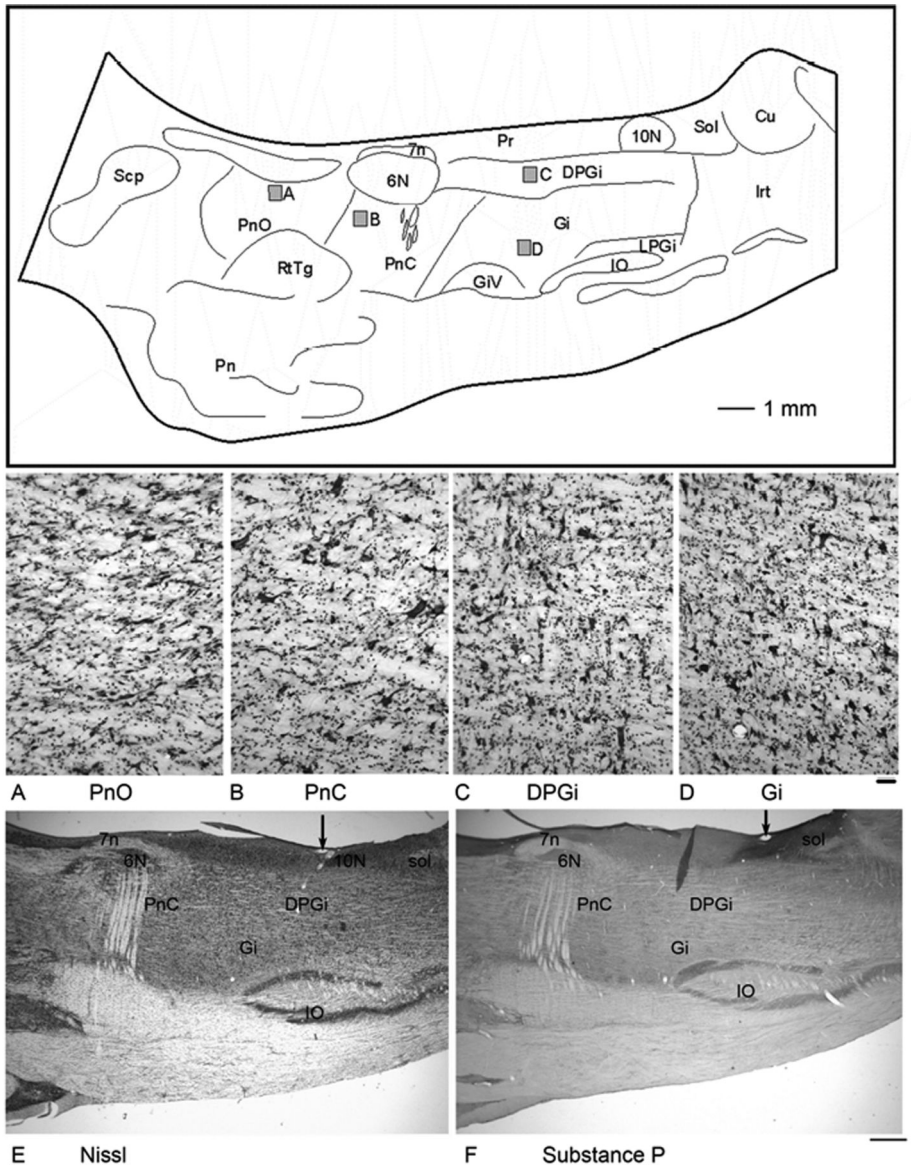

Figure 1.

A line drawing of a parasagittal section through primate PMRF showing the relative location and nuclear boundaries of PnO, PnC and Gi. The section is approximately 1.5 mm from midline. Gray boxes indicate the regions shown in high magnification photomicrographs below. A. Nissl stained photomicrograph of PnO. Note the sparse distribution of both multipolar and fusiform cells. B. Nissl stained photomicrograph of PnC showing giant cells scattered among a mixture of cells. C. Nissl stained photomicrograph of DPGi. D. Nissl stained photomicrograph of Gi.. E. Nissl-stained low-magnification photograph for a sagittal section through the PMRF. (Cresyl violet stain) F. Substance-P immunoreacted section adjacent to the

section in E. Scale bar = 50 μm (A-D), 1.0 mm (E-F). Arrows in E and F show a blood vessel used to align the sections.

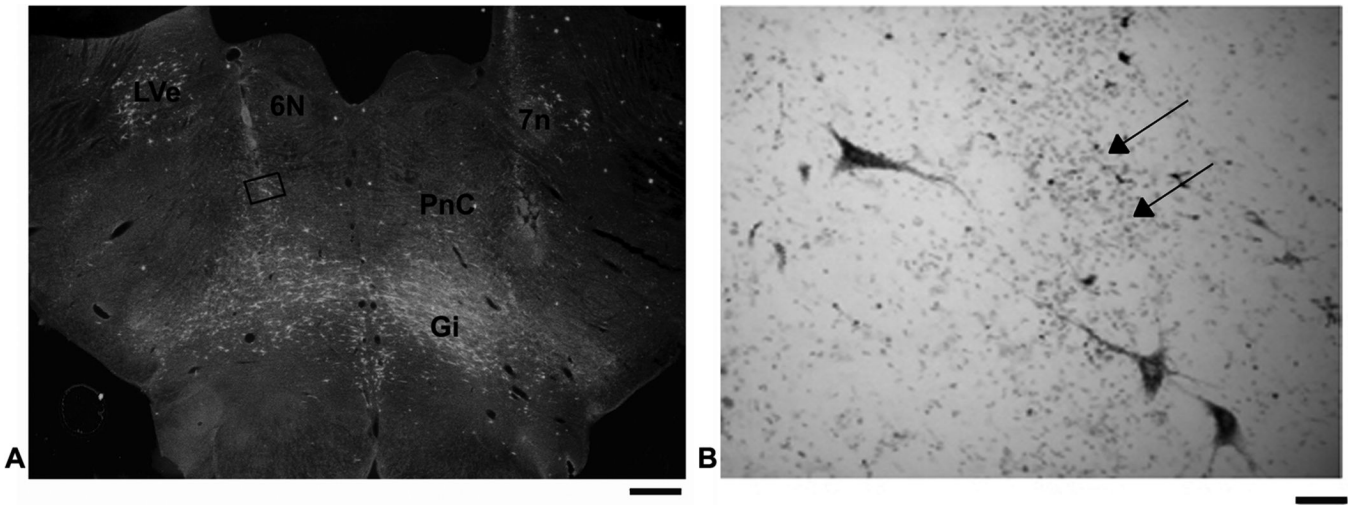

Figure 2.

A low power darkfield photomicrograph through PMRF in case M121-12 (A). Note the electrode tracks passing obliquely through the section. The greatest density of HRP labeled cells is in Gi. Boxed area in PnC is shown at higher power in B. Note the labeled cells located along the track ventral to abducens nucleus (6N). Arrows denote electrode track and associated gliosis. (neutral red counterstain) Scale bar = 1.0 mm (A) and 50μm (B).

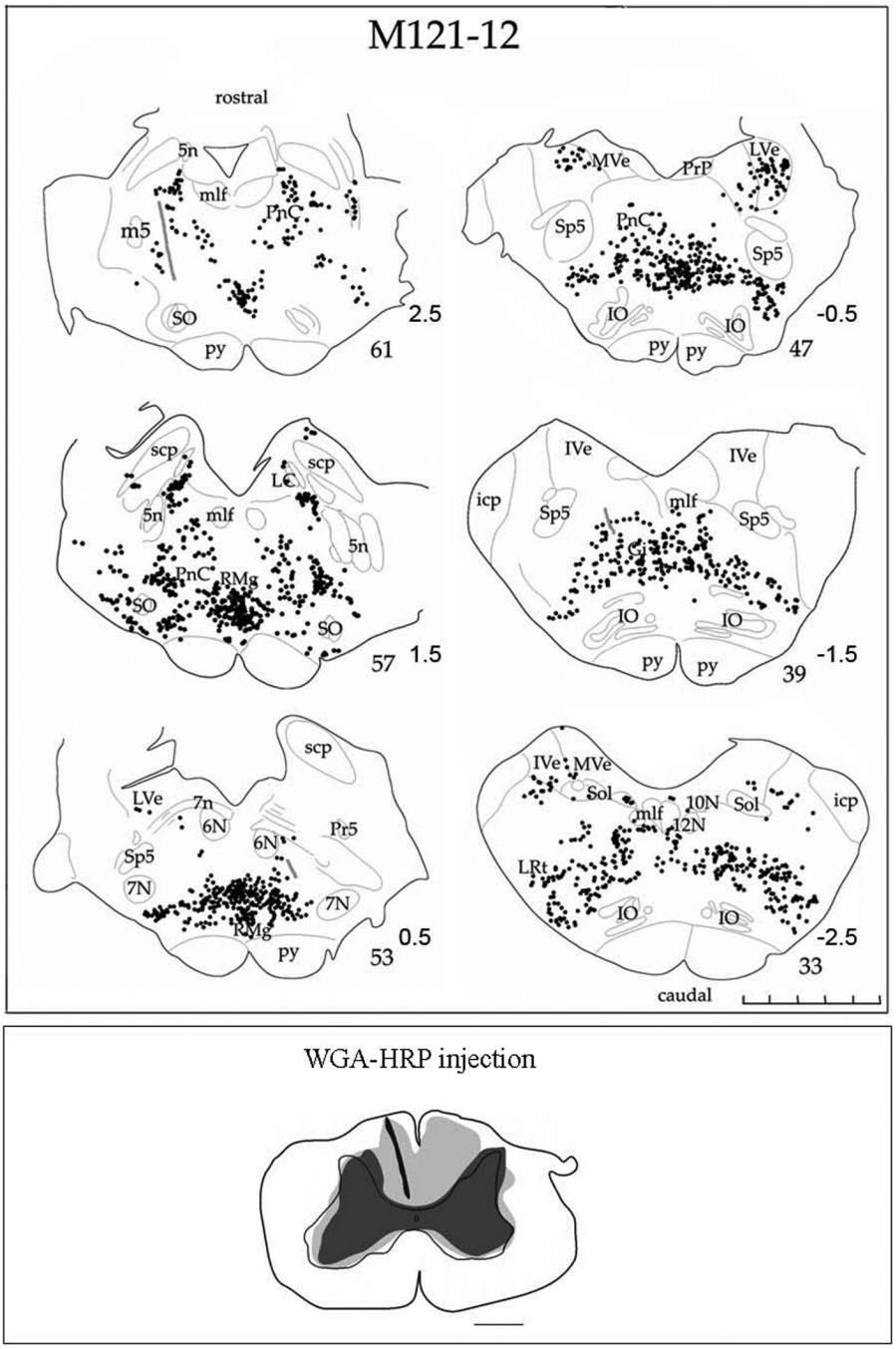

Figure 3.

Line drawings of a series of coronal sections through the PMRF in case M121-12. Multiple bilateral injections of WGA-HRP were made into the spinal cord at mid-cervical levels. Black circles indicate WGA-HRP labeled cells. Gray lines indicate electrode tracks from cell recordings made during a reaching task (Davidson and Buford, 2004; 2006). Note that the greatest density of cell labeling was found in Gi as shown in sections 39-57. The distribution of spinal cord projection neurons extends from Gi dorsally into PnC just ventral to abducens nucleus (section 53). Approximate stereotaxic coordinates ranging from +2.5 - −2.5 mm are indicated next the section numbers. The scale bar indicates 5-mm with 1-mm increments. Bottom inset shows a drawing of coronal section through the cervical spinal cord showing the

spread of the bilateral WGA-HRP injections. The blackened area indicates the needle track and the injection site core. The lighter gray regions denote lighter tracer staining corresponding to the injection halo. Scale bar= 1.0 mm

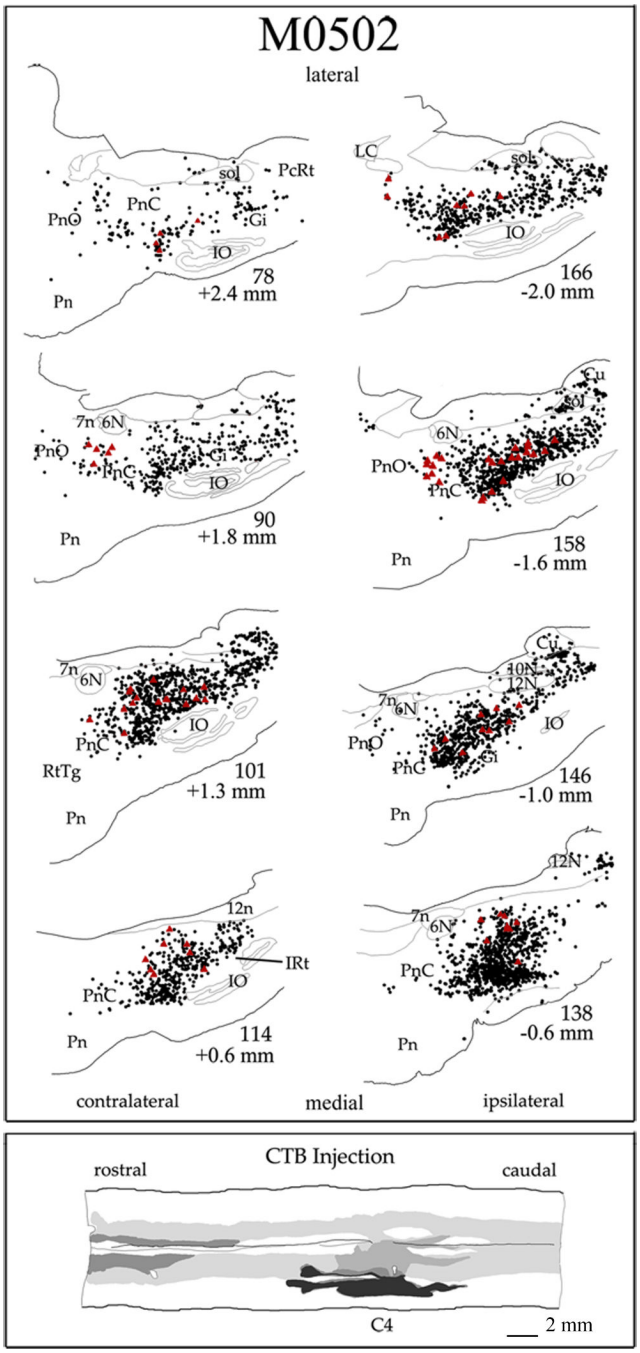

Figure 4.

Line drawings of a series of sagittal sections through the PMRF in case M0502. Sections are arranged from lateral to medial; sections contralateral to the spinal cord injections are on the left and ipsilateral is shown on the right. Approximate distance from midline is noted below the section numbers. Red triangles indicate each reticulospinal cell greater than 50 μm in diameter. Black dots indicate all other labeled CTB cells. Bottom inset contains a drawing of a horizontal section showing the extent of the CTB injections into the cervical spinal cord at levels C4. The dense core of the injection sites is shown in black and halo is shown in gray. The halo of the injection site spread to include part of the contralateral spinal cord. Scale bar = 2 mm.

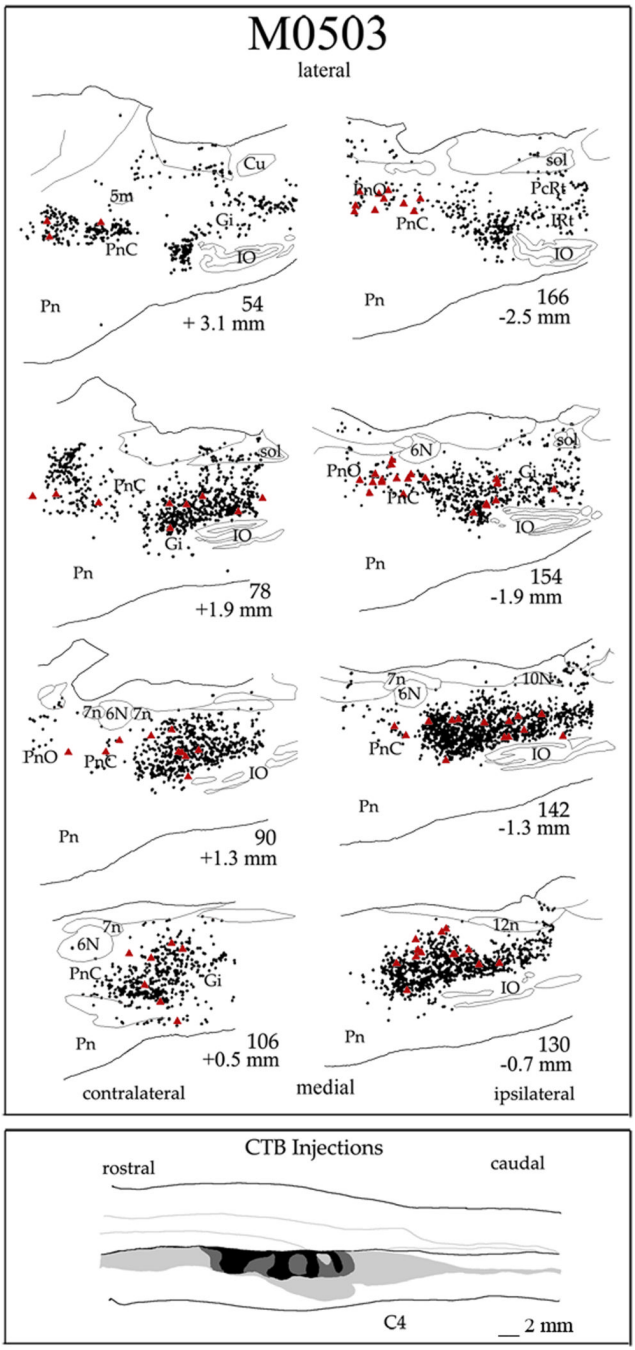

Figure 5.
Line drawings of a series of sagittal sections through the PMRF in case M0503. Details follow that described in Fig. 2

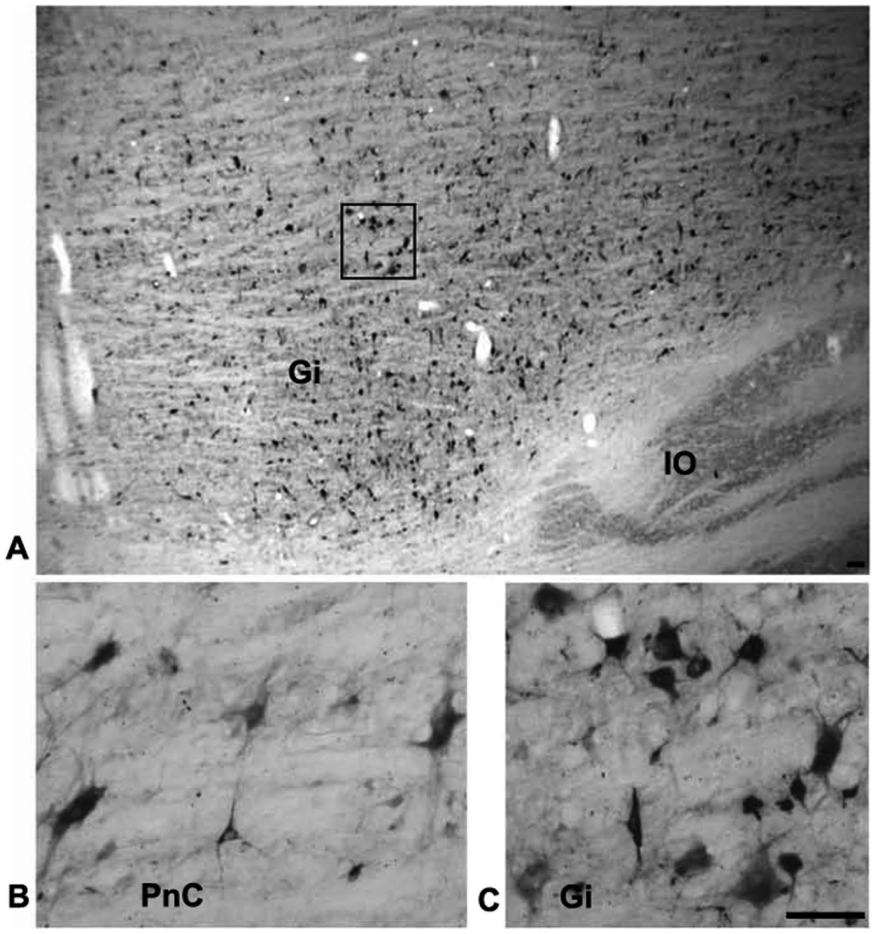

Figure 6.

Photomicrographs showing the CTB labeled reticulospinal cells. A low power photomicrograph through the ipsilateral PMRF showing CTB labeled cells in Gi in a sagittal section (A). Note that the greatest density of cell labeling is found in ventral Gi overlying the inferior olive (IO). Boxed region is shown at higher power in C. High power photomicrographs of the same section showing the labeled cells in PNc (B) and in Gi (C). Note the wide range of sizes and types of reticulospinal neurons in both B and C. Scale bar = 1.0 mm (A) and 50 μm (B & C).

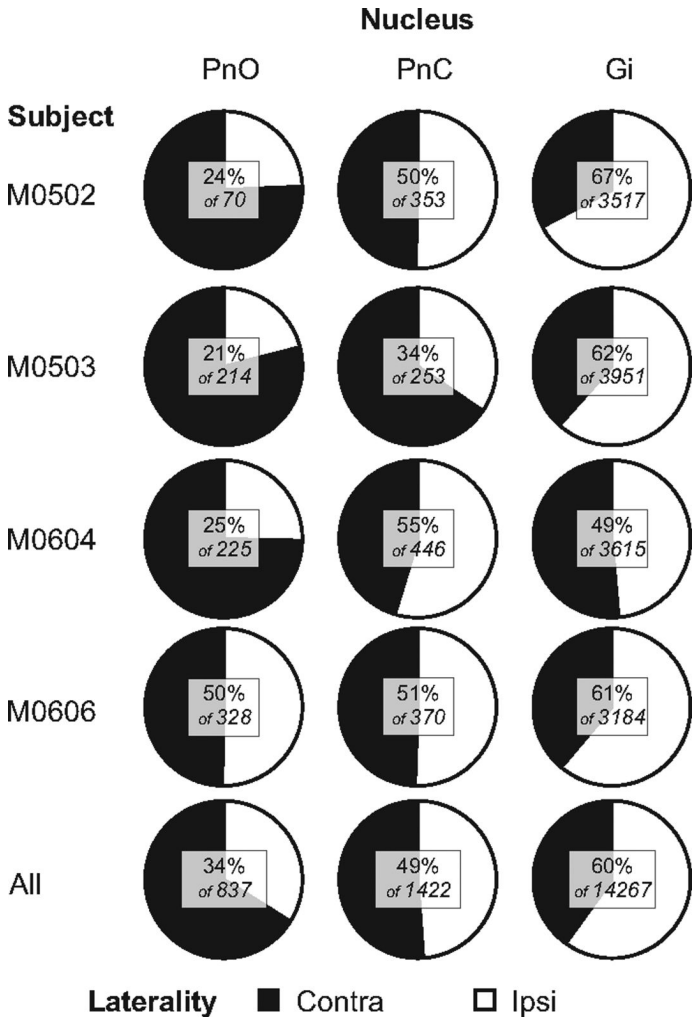

Figure 7.

Proportions of retrogradely labeled cells found in Gi, PnC, and PnO ipsilateral and contralateral to unilateral CTB injections in the spinal cord for four cases, and combined across all cases. The numbers in the inset show the percentage of ipsilateral cells as a proportion of the total number found in that nucleus. For example, across all cases, a total of 837 cells were found in PnO, and 34% of these were ipsilateral to the side of the CTB injection.